Redox Biology 47 (2021) 102162

Contents lists available at ScienceDirect

Redox Biology

journal homepage: www.elsevier.com/locate/redox

LIN28a induced metabolic and redox regulation promotes cardiac cell survival in the heart after ischemic injury

Antonia Elizabeth Yuko [a,1], Vagner Oliveira Carvalho Rigaud [a,1], Justin Kurian [a], Ji H. Lee [a], Nicole Kasatkin [a], Michael Behanan [a], Tao Wang [b], Anna Maria Luchesse [c], Sadia Mohsin [b,d], Walter J. Koch [c], Hong Wang [a], Mohsin Khan [a,e,*]

[a] Center for Metabolic Disease Research (CMDR), USA
[b] Cardiovascular Research Institute (CVRC), USA
[c] Center for Translational Medicine (CTM), LKSOM, Temple University, USA
[d] Department of Pharmacology, LKSOM, Temple University, LKSOM, Temple University, USA
[e] Department of Physiology, LKSOM, Temple University, USA

ARTICLE INFO

Keywords:
Metabolism
Myocardial ischemia
Cell therapy
Redox regulation
Survival
Oxidative stress

ABSTRACT

Rationale: Cell-based therapeutics have been extensively used for cardiac repair yet underperform due to inability of the donated cells to survive in near anoxia after cardiac injury. Cellular metabolism is linked to maintenance of cardiac stem cell (CSC) renewal, proliferation and survival. Ex vivo expansion alters (CSC) metabolism increasing reliance on oxygen dependent respiration. Whether promoting 'metabolic flexibility' in CSCs augments their ability to survive in near anoxia and repair the heart after injury remains untested.

Objective: Determine the effect of LIN28a induced metabolic flexibility on cardiac tissue derived stem like cell (CTSC) survival and repair after cardiac injury.

Methods and results: LIN28a expression coincides during heart development but is lost in adult CTSCs. Reintroduction of LIN28a in adult CTSC (CTSC-*LIN*) increased proliferation, survival, expression of pluripotency genes and reduced senescence compared to control (CTSC-*GFP*). Metabolomic analysis show glycolytic intermediates upregulated in CTSC-*LIN* together with increased lactate production, pyruvate kinase activity, glucose uptake, ECAR and expression of glycolytic enzymes compared to CTSC-*GFP*. Additionally, CTSC-*LIN* showed significantly reduced ROS generation and increase antioxidant markers. In response to H2O2 induced oxidative stress, CTSC-*LIN* showed increased survival and expression of glycolytic genes. LIN28a salutary effects on CTSCs were linked to PDK1/let-7 signaling pathway with loss of PDK1 or alteration of let-7 abrogating LIN28a effects. Following transplantation in the heart after myocardial infarction (MI), CTSC-*LIN* showed 6% survival rate at day 7 after injection compared to control cells together with increased proliferation and significant increase in cardiac structure and function 8 weeks after MI. Finally, CSTC-LIN showed enhanced ability to secrete paracrine factors under hypoxic conditions and ability to promote cardiomyocyte proliferation following ischemic cardiac injury.

Conclusions: LIN28a modification promotes metabolic flexibility in CTSCs enhancing proliferation and survival post transplantation including ability to repair the heart after myocardial injury.

Abbreviations: Cardiac tissue derived stem like cells, (CTSCs); Reactive oxygen species, (ROS); Oxygen consumption rate, (OCR); Extracellular acidification rate, (ECAR); dichloroacetate, (DCA); myocardial infarction, (MI); left anterior descending, (LAD); Pentose phosphate pathway, (PPP); 2-deoxyglucose, (2-DG); Antimycin A, (AA); Ejection fraction, (EF); Fractional shortening, (FS); Mosaic analysis with double markers, (MADM); Left ventricular internal diameter, (LVID); Left ventricular anterior wall, (LVAW).

* Corresponding author. Center for Metabolic Disease Research Assistant Professor, Department of Physiology Lewis Katz School of Medicine, Temple University, 3500 N Broad Street, MERB 454, Philadelphia, PA, 19140, USA.
E-mail address: Mohsin.khan@temple.edu (M. Khan).

[1] Both authors contributed equally.

https://doi.org/10.1016/j.redox.2021.102162
Received 18 August 2021; Received in revised form 4 October 2021; Accepted 7 October 2021

1. Introduction

The mammalian adult heart is largely dormant incapable of generating a meaningful regenerative response after injury [1]. Current therapies are designed largely to be preventive or "damage limiting", unable to regenerate lost myocardial tissue. Advent of cell-based therapies has provided hope towards replacing dead myocardium with new functional tissue with a variety of stem cells used for adoptive transfer. Studies show that the heart harbors an endogenous cell population that exhibits stem cell like properties ex vivo [2–5]. Meta-analysis of 80 preclinical studies has shown ex vivo expansion and transplantation of these cardiac tissue derived stem cells (CSCs) results in 10.7% increase in ejection fraction over placebo control after myocardial infarction [6]. Despite the success, adoptively transferred stem cells are unable to survive in the ischemic cardiac environment with less than 1% cells surviving 24 h post transplantation [7] suggesting need for strategies that enhance effectiveness of cell-based therapies.

Cardiac ischemic injury is associated with decreased oxygen levels in the heart that provides a hostile environment for adoptively transferred stem cells [8,9]. Cell-based therapies typically rely on ex vivo expansion of stem cells under ambient oxygen prior to transplantation that favors oxidative phosphorylation [10,11]. Donated stem cells are exposed to ischemic cardiac milieu composed of near anoxia, increased ROS and pro-inflammatory factors that together push massive cell loss upon transplantation. Recent studies have shown metabolism as a critical determinant of stem cell fate regulating various processes such as cell proliferation [12], survival [13], and commitment [14]. Metabolic signaling pathways are sensitive to changes in environmental conditions allowing stem cells to adapt to fluctuating oxygen and nutrient levels [15]. Interestingly, developmental tissue harbors pluripotent stem cells that possess a specialized metabolic state linked to increased proliferation and regeneration potential [16]. Similarly, adult stem cells reside in hypoxic niches and prefer glycolysis for maintenance of stemness [17,18] but ex vivo expansion alters metabolic properties of the cells. Identification of developmental metabolic regulators and their reintroduction in adult stem cells may provide 'metabolic flexibility' promoting survival after ischemic injury. We previously identified developmental microRNA-294 signaling complex active in the heart that shuts down with cardiac maturation [19]. miR-294 signaling pathway includes LIN28a, a master regulator of growth and metabolism. Reintroduction of LIN28a in adult tissue reprograms cellular metabolism and promotes regeneration after injury. We have recently identified a new cardiac tissue derived stem like cell (CTSC) in the heart with unique transcriptome compared to all other known and cardiac and other stem cell types [2]. CTSCs express LIN28a in the neonatal heart but not in the adult. Whether reintroduction of LIN28a in the adult cells reprograms metabolism enhancing survival post transplantation in the adult heart after injury was not tested and remains unknown.

In this article, we report therapeutic efficacy of LIN28a for enhancing cardiac repair potential of novel cardiac tissue derived stem like cells (CTSCs). LIN28a engineered CTSCs (CTSC-*LIN*) show enhanced glycolytic metabolism, proliferation and survival in response to oxidative stress. When transplanted into an infarcted myocardium, CTSC-*LIN* showed increased persistence and proliferation along with reduced apoptosis 2 days after transplantation together with improvement of cardiac structure and function 8 weeks after injury. Our results here show metabolic reprogramming of CTSCs by LIN28a as a novel strategy to enhance post transplantation survival in the heart after injury.

2. Methods

2.1. Cell isolation, culture and lentiviral modification

Cardiac derived stem like cells (CTSCs) are isolated from the hearts of C57BL/6 Mice (Jackson) as described previously [2]. Briefly, hearts were minced in small pieces and digested in collagenase at 150U mg/ml (Worthington Bio Corp, Lakewood, NJ) for 2 h at 37 °C. After myocyte removal at low-speed centrifugation, the cells are then passed through 100 μm and 50 μm filters (BD biosciences CA), centrifuged at 1200 rpm for 5 min, with resuspension of the pellet in CTSC media consisting of DMEM-F12 (Gibco), 10% Embryonic Stem Cell Fetal Bovine Serum (Gibco), 1% Penicillin-Streptomycin-Glutamine (PSG) (Gibco), 1x Insulin-Transferrin-Selenium (Gibco), Recombinant Human-EGF 10 ng/mL (Peprotech), Recombinant Human-FGF 10 ng/mL (Peprotech), and Leukemia Inhibitory Factor (Millipore Sigma), and incubated in a 37 °C 5% CO_2 incubator. Supernatant was replated 24hrs later in a dish to remove fast adhering cells. CTSCs are infected with Lv-PGK1-LIN28a (CTSC-*LIN*) and green fluorescent protein (GFP) lentivirus (CTSC-*GFP*) to create stable cell lines kept between passages 15–22 to minimize variation. Additional details provided in the online data supplement.

2.2. Cell viability and proliferation assays

Cell viability is assessed by trypan blue exclusion method in serial subcultures of CTSCs. DNA content is assessed by CyQuant, metabolic activity with 3-(4,5Dimethylthiazole-2-yl)-2,5-diphenytetrazolium bromide (MTT) and Resazurin assay of CTSCs by individually plating 2000 cells/well in 6 replicates/time point in different 96-well plate followed by incubation with CyQuant (Invitrogen), 3-(4,5Dimethylthiazole-2-yl)-2,5-diphenytetrazolium bromide (ATCC) and resazurin (CST). Population doubling time is calculated using cell counts in serially sub-cultured cells as described previously [2,20].

2.3. Seahorse assays

A seahorse Bioscience XF96 extracellular flux analyzer is utilized to measure oxygen consumption rates (OCR) and extracellular acidification rates (ECAR) in both CTSC-*LIN* and CTSC-*GFP* using the mito stress and glycolysis stress kit (Agilent Technologies) respectively. Cell energy phenotype is assessed using the cell energy phenotype test kit (Agilent Technologies) using a seahorse bioanalyzer.

2.4. Metabolomics

CTSC-*LIN* and CTSC-*GFP* were cryopreserved and were sent to Metabolon Inc. for biochemical extraction and analysis by liquid chromatography and high-resolution tandem mass spectrometry (LC-MS/MS) on Metabolon's Global Platform. Using proprietary software, raw data were extracted, peak-identified, and processed by Metabolon.

2.5. Pyruvate, pyruvate kinase, lactate and glucose uptake assays

CTSCs were grown to confluency followed by preparation for measurement of lactate (Biovision), pyruvate (Abcam), glucose uptake (Life technologies) and pyruvate kinase activity (Biovision) for both cell types according to manufacturer's protocol.

2.6. Flow cytometry based cell survival assay

Cell death is measured by Annexin-V staining (BD Bioscience) in CTSCs treated with hydrogen peroxide according to manufacturer's protocol. Flow cytometry is performed on BD LSRII flow cytometer (BD Bioscience).

2.7. Pharmacological treatments

CTSC were treated with 3-Bromopyruvate (Sigma Aldrich), dichoroacetate (DCA, Sigma Aldrich), antimycin A (Sigma Aldrich) and 2-deoxyglucose (Sigma Aldrich).

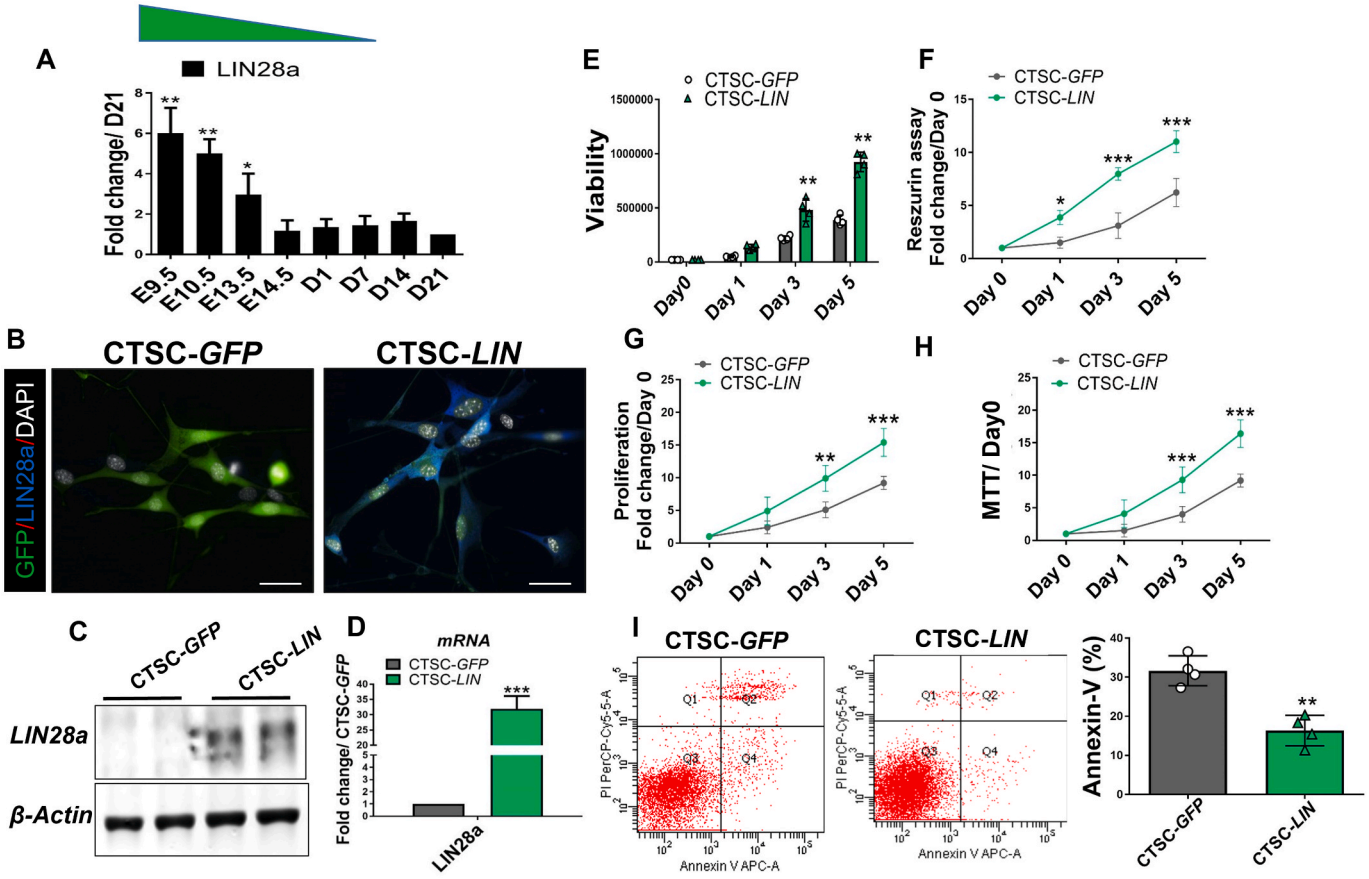

Fig. 1. LIN28a modification promotes viability, growth kinetics and survival under oxidative stress in CTSCs. A) Temporal expression of LIN28a in the embryonic (E9.5, 10.5, 13.5, 14.5), postnatal (D1, D7) and adult heart (D14, D21) declines with age. (n = 4). B) CTSC express LIN28a along with GFP with no expression in control GFP only cells. GFP (green), LIN28a (Blue), Nuclei (white). Scale bar = 40 μm. C) Immunoblot validation of LIN28a expression after lentiviral modification in adult CTSC. (n = 3). D) mRNA expression of LIN28a in modified CTSCs compared to control cells (n = 3). E) Increased viability in CTSC-*LIN* at day 3 and day 5 after plating compared to CTSC-*GFP* (n = 6). F and H) Resazurin assay and MTT shows increased metabolic activity in CTSC-*LIN* compared to control respectively (n = 6). G) Increased DNA content in CTSC-*LIN* compared to CTSC-*GFP* as measured by CyQuant (n = 6). I) Decreased population doubling time in CTSC-*LIN* compared to CTSC-*GFP* (n = 6). J) Flow cytometry-based measurement of cell survival show decreased % of Annexin-V+ cells in CTSC-*LIN* compared to control cells (n = 5). CTSC-*LIN* vs CTSC-*GFP* *$p<0.05$, **$p<0.01$, ***$p<0.001$. (For interpretation of the references to color in this figure legend, the reader is referred to the Web version of this article.)

2.8. Immunoblots

Immunoblot analysis is performed as described previously [2,19] with additional detail in online data supplement.

2.9. Immunostaining

Immunocytochemistry, TUNEL assays, EdU labeling assay and immunohistochemistry are performed as described previously with additional detail in online supplement including a list of antibodies in Online Table II.

2.10. Measurement of mitochondrial membrane potential by TMRM

For measurement of mitochondrial membrane potential, 50,000 cells/wells were plated into 2-chamber slide for each CTSC line. Final concentration of 50 nM TMRM (Invitrogen) prepared in CTSC growth medium, was added to samples and incubated for 30 min at 37 °C. Live nuclear dye (Invitrogen) was added to chambers 10 min prior to scanning on the microscope. Images were taken on Leica SP8 Confocal Microscope. TMRM intensity quantifications were done through ImageJ.

2.11. Animal studies

All mice (C57BL/6; 8–12 weeks old male mice) used in this study were obtained from The Jackson Laboratories (Bar Harbor, ME). All surgical procedures and animal care protocols were approved by the Temple University Animal Care and Use Committee.

Myocardial infarction. Mice underwent surgery to ligate the left anterior descending coronary artery as reported previously [21,22] followed by administration of PBS (n = 25), CTSC-*GFP* (n = 25) or CTSC-*LIN* (n = 25) suspended in PBS intramyocardially into the left ventricular wall (border zone) at four different locations immediately after left anterior descending ligation. Tissue was harvested at 2, 7 days and 8 weeks after AMI for histological analysis.

Acute myocardial infarction (AMI) was induced as described previously. Briefly, mice are anesthetized with a mixture of 1.5% isoflurane and oxygen (1 L/min), orally intubated and placed in a supine position. Respiration is controlled by mechanical ventilation using a rodent ventilator (Nemi Scientific, Inc., Framingham, MA) with tidal volume set to 0.4 mL at a rate of 110 strokes/min. The chest is then shaved, cleaned free of hair and sterilized. Under a dissecting microscope, a left thoracotomy is performed in the fourth intercostal space. Heart always resided in the thoracic cage and was visualized by using a clamp. After displacing the pericardium, an 8-0 monofilament nylon suture on a curved tapered needle is passed under the left anterior descending

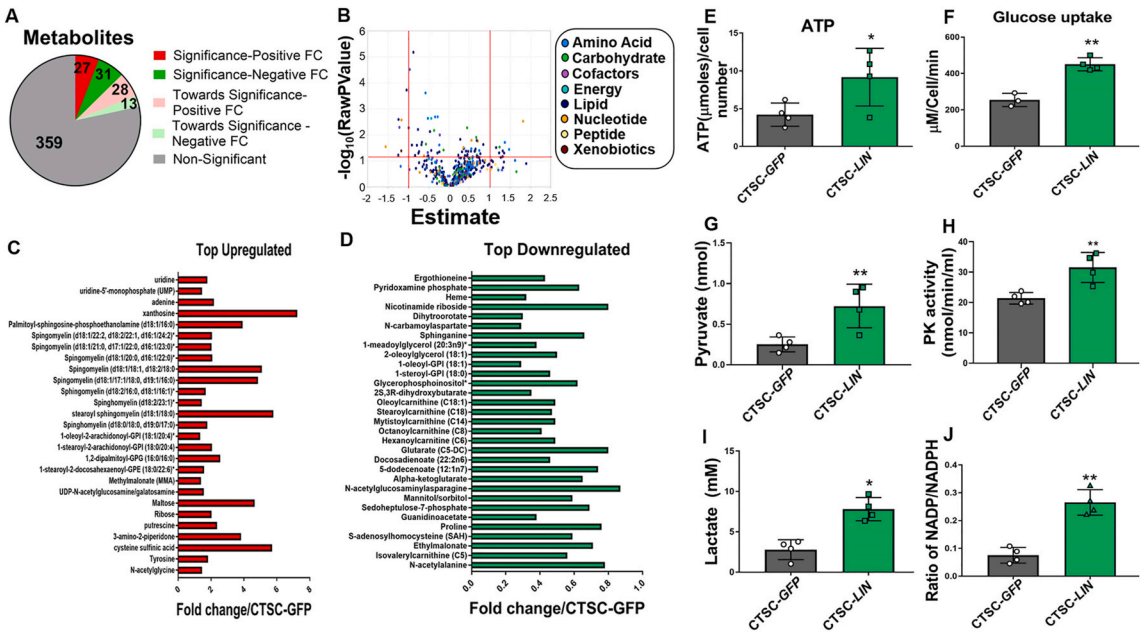

Fig. 2. Metabolomic analysis of CTSCs modified with LIN28a. A) Global profiling of significant positive/negative metabolites and towards significance positive/negative metabolites in CTSC-*LIN* (n = 6). B) Volcano plot shows significantly altered metabolites (n = 6). C-D) Top upregulated and downregulated metabolites in CTSC- *LIN* compared to CTSC-*GFP* (n = 6). E) ATP quantification assay shows increased ATP production in CTSC-*LIN* compared to controls (n = 4). F) Increased glucose uptake in CTSC-*LIN* compared to CTSC-GFP as measured by glucose uptake assay kit. (n = 4). G) CTSC-*LIN* exhibit increased intracellular pyruvate levels as compared to CTSC-*GFP* as measured by pyruvate measurement kit (n = 4). H) Increased activity of pyruvate kinase in CTSC-*LIN* compared to CTSC-*GFP* determined by pyruvate kinase assay kit (n = 4). I) Enhanced intracellular lactate production in nCTSC compared to CTSCs and aCTSC as measured by lactate detection kit (n = 4). J) Ratio of NADP/NADPH is increased in CTSC after LIN28a modification compared to control cells. (n = 4). CTSC-*LIN* vs CTSC-*GFP* $*p<0.05$, $**p<0.01$, $***p<0.001$.

coronary artery (LAD) 4 mm below the left atrium and permanently tied to eliminate blood flow distal to the suture. Pericardium is re-draped by gently pulling it over the heart with forceps, and the chest was then closed following the injection. A 22-gauge syringe was used to re-establish negative pressure within the chest cavity prior to extubation. Cells were injected within 30sec of LAD ligation, in a total volume of 100 μl, four intramyocardial injections in four injections sites (25 μl/site) all around the left ventricular border zone area visible by epicardial blanching or color change following LAD ligation. LAD and epicardial blanching are then visualized by looking through a surgical microscope. Animals received post-surgical pain management with buprenorphine and surgical inflammation control with meloxicam. Animals were recovered until freely mobile on a heating pad at which point they were then placed into a clean cage and housed for the duration of the experiment.

Mini-Osmotic pump implantation. Osmotic minipumps (Alzet; Cupertino, CA) are loaded with solution containing 39.0625 mg/mL EdU (Life Technologies, Carlsbad, CA) dissolved in 50/50% mixture of DMSO/ddH2O. Pumps are prepared as previously described [23] and implanted subcutaneously between the two scapulae at the time of MI surgery. The minipumps deliver a continuous infusion of EdU over the course of 1 week, and after 1 week all pumps are removed.

2.12. Statistics

Statistical analysis is performed using unpaired Student's *t*-test for data comparing 2 groups and 1-way or 2-way ANOVA with Bonferroni post-hoc test for comparing more than 2 groups for data exhibiting normal distribution and Dunnett post hoc test for comparison of 2 or more groups with the control group. For data that do not exhibit normal distribution Mann-Whitney test was used. All data sets were assessed for normality using Shapiro-Wilk test for normality. $P < 0.05$ is considered statistically significant. Error bars represent ±SD. Statistical analysis is performed using Graph Pad prism v 7.0 software.

3. Results

Temporal expression of LIN28a in the heart in response to homeostatic changes. LIN28a is a primal regulator of pluripotency, expressed in various tissues during development [24]. Reintroduction of LIN28a in adult tissues leads to robust regenerative response [25]. Nevertheless, there is limited evidence for LIN28a in the context of cardiac biology. Previously, we have shown that embryonic stem cell cycle miR-294 promotes LIN28a expression in cardiac cells [19]. Here we show that miR-294 mimic treatment upregulates LIN28a in neonatal (Online Fig. 1A) and adult cardiomyocytes (Online Fig. 1B) together with increased LIN28a expression in the heart administered with miR-294 mimic 2 days after delivery (Online Fig. 1C). Cardiac tissue derived stem like cells (CTSCs), a novel cardiac cell population previously identified [2], overexpressing miR-294 show increased LIN28a expression, which is reduced in response to treatment with antogomiR-294 (Online Fig. 1D). The main question was whether LIN28a is expressed in the heart during physiological cardiac growth and pathological stress. For this purpose, samples from embryonic, postnatal and adult cardiac tissue were analyzed for expression of LIN28a. Increased LIN28a mRNA expression was observed in the heart during early embryonic development followed by rapid decline in the postnatal and adult cardiac tissue (Fig. 1A and Online Fig. 1E). Next, LIN28a expression was assessed in the heart after myocardial injury. Increased expression of LIN28a was observed in the border zone area of wild type mice 2 days after LAD ligation (Online Fig. 1F). Ischemia-reperfusion (I/R) injury increased LIN28a after 1 day which not significant and is lost by day 7 while *trans*-aortic constriction (TAC) at 3 and 9 weeks significantly blunts LIN28a expression (Online Fig. 1G). Collectively, our results show that LIN28a expression in the heart coincides with early cardiac development and is lost with maturation. Injury to the heart acutely increased LIN28a expression which is lost early with progressing adverse remodeling of the cardiac tissue.

LIN28a modified CTSCs exhibit increased growth kinetics,

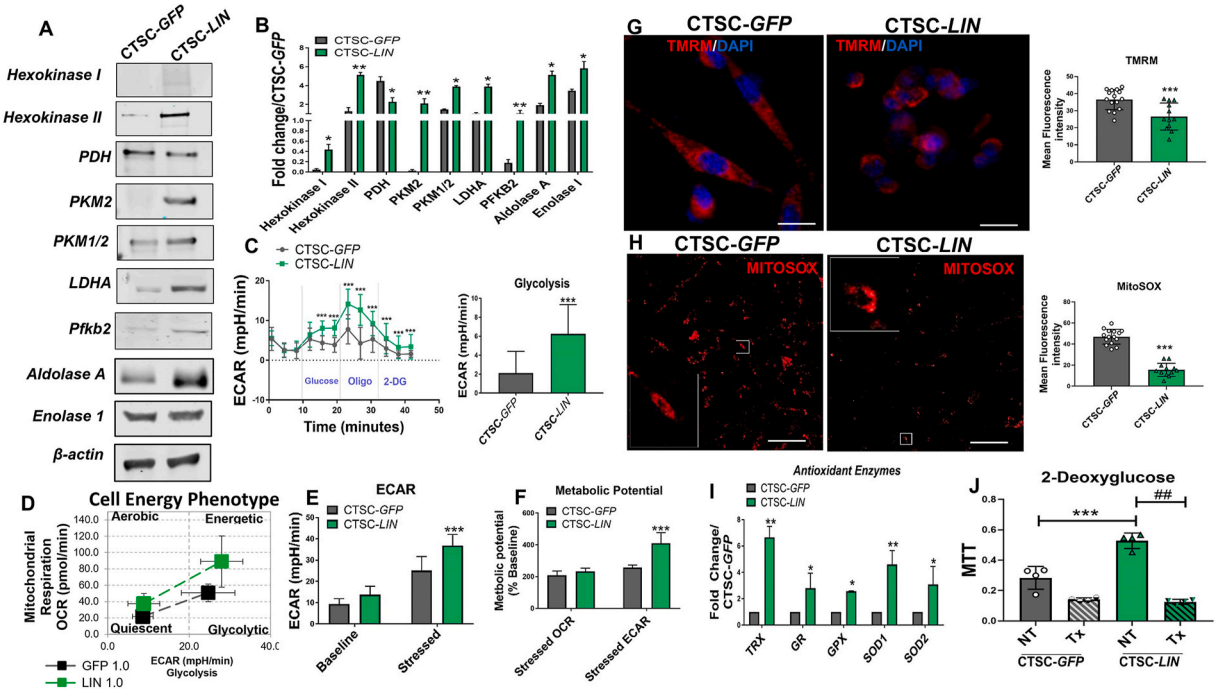

Fig. 3. Enhanced cellular bioenergetics, low membrane potential and reduced ROS levels in CTSCs after LIN28a modification. A) Immunoblot analysis of glycolytic enzymes in CTSC-LIN and CTSC-*GFP* along with quantification (B) (n = 3). C) Measurement of extracellular acidification rates (ECAR) by seahorse bioanalyzer show increased ECAR and glycolysis in CTSC-*LIN* compared to CTSC-*GFP* (n = 15 replicates/line/3 independent experiments) 48hrs after plating. Data for ECAR was normalized to cell number and protein content. D-F) Measurement of metabolic potential and stressed phenotype using seahorse cell energy phenotype test kit (n = 15 replicates/line/3 independent experiments 48hrs after plating. G) CTSC-*LIN* demonstrate low mitochondrial membrane potential visualized by TMRM staining while CTSC-*GFP* have high TMRM intensity. TMRM (red), nuclei (blue), Scale bar = 20 μm (n = 4). H) Reduced MitoSOX intensity in CTSC-*LIN* compared to CTSC-*GFP*. Scale bar = 40 μm (n = 4). I) Increased mRNA expression of antioxidant markers in CTSC-*LIN* compared to control. (n = 4). J) Reduced metabolic activity in CTSC-*LIN* 48hrs after treatment with 2-deoxyglucose as measured by MTT assay. (n = 4). CTSC-*LIN* vs CTSC-*GFP* $*p<0.05$, $**p<0.01$, $***p<0.001$. (For interpretation of the references to color in this figure legend, the reader is referred to the Web version of this article.)

survival in response to oxidative stress and a youthful phenotype. We have previously identified CTSCs in the heart as a novel cardiac cell population and analysis of CTSCs from 2-day old mouse heart shows increased expression of LIN28a [2]. Adult CTSC from 2-month-old and aged CTSC from 2-year-old heart do not express LIN28a [2]. Therefore, in order to test whether reintroduction of LIN28a in adult CTSC is beneficial, we decided to genetically modify CTSC with LIN28a. Using a lentivirus carrying LIN28a together with green fluorescent protein (GFP), CTSCs from adult heart were engineered to express LIN28a (CTSC-*LIN*), confirmed by immunocytochemistry (Fig. 1B), immunoblot (Fig. 1C) and qRT-PCR (Fig. 1D). CTSCs engineered with GFP only (CTSC-*GFP*) lentivirus was used as controls. Cell lines expressing similar LIN28a expression were generates, validated by immunoblot analysis (Online Fig. 1H) and further used for experiments. Analysis of viability showed that CTSC-*LIN* have increased viability (Fig. 1E) together with enhanced DNA content (Fig. 1G) and metabolic activity (Fig. 1F and H) compared to CTSC-*GFP*. Next, CTSC-*LIN* were assessed for their ability to resist H2O2 induced oxidative stress. Reduced number of Annexin-V+ cells were observed in CTSC-*LIN* compared to control cells as confirmed by FACS based cell death assay (Fig. 1I) together with increased AKT^{S473} phosphorylation under stress from H2O2 (Online Fig. 1I). Finally, whether LIN28a introduction in adult CTSCs promotes a youthful phenotype was assessed. Increased expression of pluripotent markers Nanog and Sox 2 was observed in CTSC-*LIN* compared to CTSC-*GFP* as measured by immunocytochemistry (Online Fig. 2A and B) together with upregulation of markers of pluripotency as confirmed by qRT-PCR (Online Fig. 2C). Concurrently, CTSC-*LIN* demonstrated reduced senescence associated β-galactosidase staining compared to CTSC-*GFP* (Online Fig. 2D). Taken together, reintroduction of LIN28a in adult CTSCs enhances proliferation and survival together with induction of youthful phenotype compared to control cells.

LIN28a promotes energetic activity by increasing both oxidative phosphorylation and glycolysis in adult CTSCs. Metabolism has been shown recently as a critical determinant of stem cell fate and function [26]. Since LIN28a is a master regulator of cellular metabolism [25], whether reintroduction of LIN28a in adult CTSCs alters metabolism was assessed. For this purpose, samples from CTSC- *LIN* and CTSC-*GFP* were sent for metabolomics. Results identified a total of 458 metabolites analyzed in both types of CTSC samples (Online Fig. 3A) with 27 metabolites significantly upregulated while 31 downregulated in CTSC-*LIN* compared to CTSC-*GFP* (Fig. 2A and B). Top upregulated and down regulated metabolites in CTSC-*LIN* compared to control cells (Fig. 2C and D) indicate various glycolytic intermediates to be elevated. Several metabolites in the pentose phosphate pathway (PPP) were elevated while pyrimidine synthetic intermediates were low in CTSC-*LIN* compared to control cells indicating increased shunting through the PPP to support high nucleotide production required for highly proliferative cells. In contrast, downstream TCA cycle including α-ketoglutarate were lower in CTSC-*LIN* compared to control cells. Interestingly, there was robust increased in several sphingolipids in CTSC-*LIN* compared to control cells. Finally, CTSC-*LIN* showed elevated levels of metabolites involved in glutathione cycling compared to control cells. To further validate results of metabolomics, several invitro metabolic measurements were done in both CTSC-*LIN* and CTSC-*GFP*. Measurement of ATP showed increased levels in CTSC-*LIN* compared to control cells (Fig. 2E). CTSC-*LIN* showed increased glucose uptake (Fig. 2F) together with elevated pyruvate (Fig. 2G), pyruvate kinase activity (Fig. 2H) and lactate production (Fig. 2I) suggesting increased glycolytic flux in CTSC-*LIN*. Moreover, NADP/NADPH ratio was significantly higher in CTSC-*LIN* compared to control cells corroborating metabolomics data for increased PPP flux in CTSCs after LIN28a modification.

Next, levels of various metabolic enzymes were analyzed in both

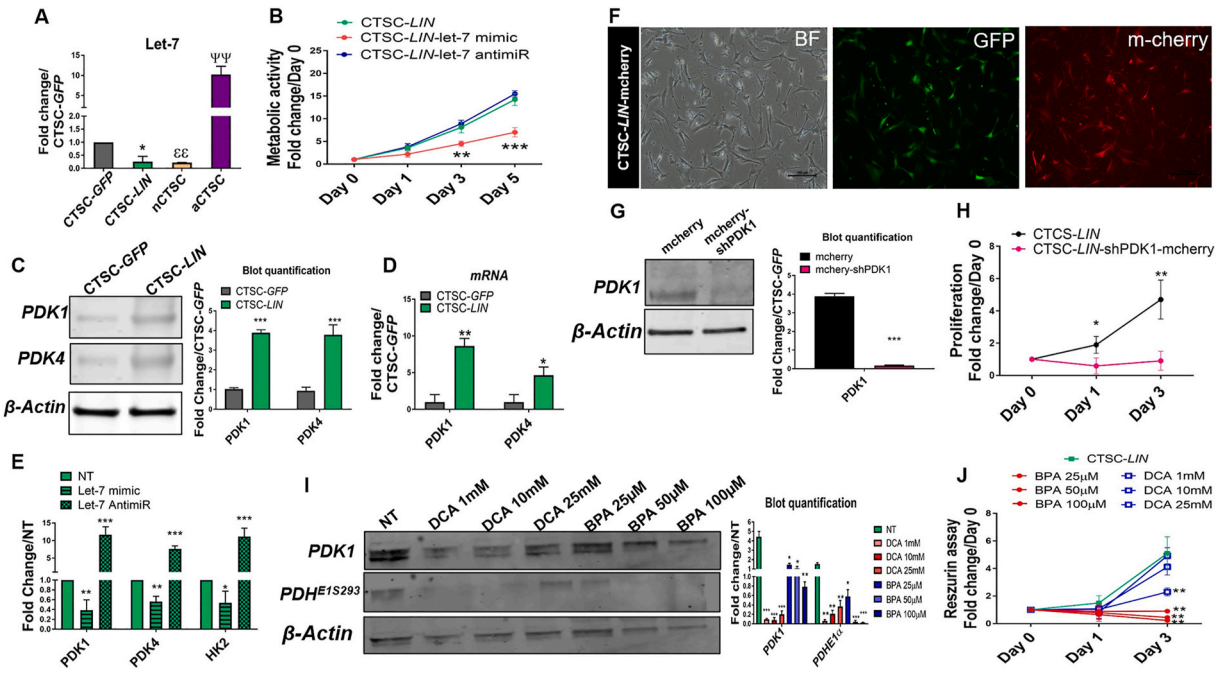

Fig. 4. LIN28a salutary effects on CTSC function are mediated by let-7 dependent effects. A) Let-7 expression in CTSC-LIN and CTSC-GFP. (n = 3) B) MTT activity in CTSC-LIN treated with let-7 mimic and antimiR at day 1, 3, and day 5 after treatment. (n = 6). C) Increase protein expression of *PDK1* and *PDK4* in CTSC-LIN compared to control along with blot quantification. (n = 3). D) mRNA expression of *PDK1* and *PDK4* CTSC-*LIN* and CTSC-*GFP*. (n = 3). E) mRNA expression of PDK1, PDK4 and HK2 in CTSC-LIN 72hrs after let-7 mimic and antimiR treatment. (n = 5). F) Immunofluorescence validation of *PDK1* lentiviral knockdown with mcherry-shPDK1. GFP (green) and mcherry-shPDK1 (red). Scale bar = 100 μm. G) Immunoblot validation of PDK1 knockdown in CTSC-*LIN* along with quantification 96hrs after shPDK1 treatment. H) Decreased proliferation in CTSC-LIN-shPDK1-mcherry cells compared to CTSC-*LIN* at day 1 and 3 as measured by CyQuant assay (n = 4). I) Increased PDK1 and PDHE1α^{S293} phosphorylation is reduced by 48hrs after treatment with 3-bromopyruvate (BPA) and dichloroacetate (DCA). J) Decreased viability in CTSC-*LIN* treated with BPA and DCA at day 1 and day 3 as measured by resazurin assay. (n = 4). CTSC-*LIN* NT vs Tx $*p<0.05$, $**p<0.01$, $***p<0.001$. (For interpretation of the references to color in this figure legend, the reader is referred to the Web version of this article.)

CTSC-*LIN* and CTSC-*GFP*. Immunoblot analysis identified increased levels of glycolytic enzymes such as *HKI, HKII, PKM2, PKM1/2, LDHA, PFKB2, Aldolase A* and *Enolase 1* in CTSC-*LIN* compared to control cells (Fig. 3A and B) in parallel to increase mRNA expression of glycolytic enzymes (Online Fig. 3B) and increased fatty-acid metabolism genes (Online Fig. 3C). Cellular bioenergetics was measured in both CTSC-*LIN* and CTSC-*GFP* using seahorse bioanalyzer. Increased ECAR, glycolysis and glycolytic capacity was observed in CTSC-*LIN* compared to CTSC-*GFP* (Fig. 3C). Interestingly, OCR, ATP production and maximum respiration was also found to be increased in CTSC-*LIN* compared to control cells (Online Fig. 3D), a phenotype reflective of cell undergoing rapid proliferation. Next, metabolic potential of adult CTSCs after LIN28a modification was analyzed by measuring ECAR and OCR under normal and stressed conditions simultaneously. Results showed that LIN28a modification shifted adult CTSCs from a quiescent to a more energetic phenotype with increases in both ECAR and mitochondrial function (Fig. 3D). Under stressed condition, CTSC-*LIN* increase ECAR rates compared to control cells (Fig. 3E and F) further highlighting metabolic flexibility in the CTSCs after LIN28a modification. Collectively, LIN28a modification of adult CTSCs reprograms cellular metabolism towards aerobic glycolysis for rapid energy production that supports increased proliferation rates.

Mitochondrial function, membrane potential and redox regulation under oxidative stress in LIN28a modified CTSCs. These set of studies were designed to profile mitochondrial function in adult CTSCs after modification with LIN28a. Analysis of mitochondrial content indicates increased mtDNA content (Online Fig. 3E) and citrate synthase activity (Online Fig. 3F) in CTSC-*LIN* compared to control cells. In parallel, mitochondrial membrane potential (ΔΨm) was significantly lower in CTSC-*LIN* compared to control cells as measured by TMRM (Fig. 3G). Next, levels of reactive oxygen species and antioxidant signaling was tested in CTSC-*LIN*. Results showed that CTSC-*LIN* have significantly lower MitoSOX levels compared to CTSC-*GFP* in response to H2O2 stress (Fig. 3H) together with increased expression of antioxidant genes such as *TPX, GR, GPX, SOD1* and *SOD2* CTSC-*LIN* compared to control cells (Fig. 3I). The next question was to determine how LIN28a modification alters CTSC metabolism in response to H2O2 induced stress. For this purpose, CTSC-*LIN* and CTSC-*GFP* cells were treated with H2O2 for 2hrs followed by RNA analysis for glycolytic enzymes. Results show that CTSC-*LIN* have significantly higher ability to upregulate glycolytic enzymes compared to CTSC-*GFP* under stress (Online Fig. 4A and B). Finally, whether blocking metabolic flux alters CTSC proliferation rates was assessed. CTSC-*LIN* and CTSC-*GFP* were treated with antimycin A (AA), an inhibitor of oxidative phosphorylation and 2-deoxyglucose (2-DG) that inhibits glycolytic flux. Results show increased susceptibility of CTSC-*LIN* to 2-DG (Fig. 3J) treatment resulting in significant decline in cell proliferation while no change was observed after AA (Online Fig. 4C) treatment compared to CTSC-*GFP*.

LIN28a functional changes are linked to Let-7/PDK1 pathway in CTSCs. The main question was to determine the mechanism behind LIN28a mediated salutary effects on CTSC function. Studies have shown that LIN28a represses let-7 expression thereby regulating gene expression of let-7 target genes [27]. let-7 expression was found to be increased in CTSCs with age while LIN28a modification reduced expression in adult CTSCs (Fig. 4A). Next, we tested whether increased proliferation rates in CTSC-*LIN* are dependent on let-7. For this purpose, CTSC-*LIN* were treated with let-7 mimic and antimiR. Results showed significantly decreased proliferation in CTSC-*LIN* after treatment with let-7 mimic compared to non-treated cells while let-7 antimiR showed slight increase in proliferation that was not significant as measured by MTT assay (Fig. 4B). To identify downstream let-7 metabolic target genes, we conducted a miRNA-let-7 target prediction search using targetscan 7.2

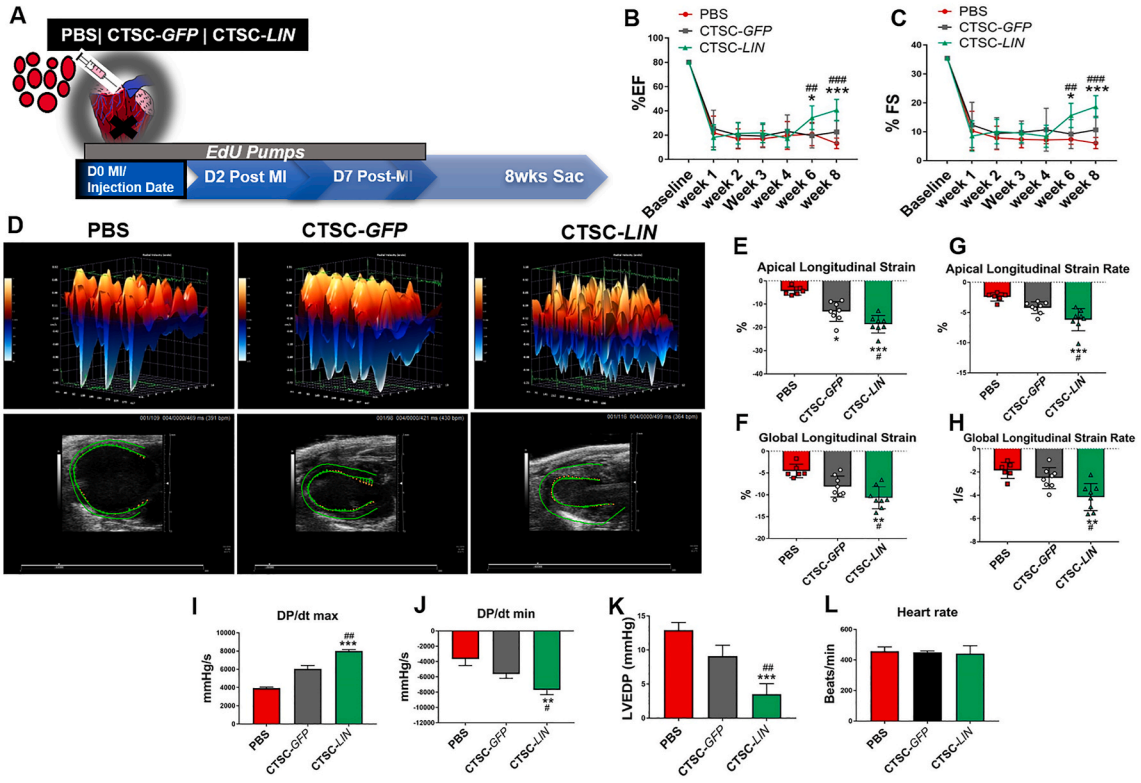

Fig. 5. Enhanced cardiac function in CTSC-*LIN* transplanted mice 8 weeks after myocardial ischemic injury. A) Schematic illustration of experimental design. Animals were divided into 3 groups and administered PBS (n = 25), CTSC-*GFP* (n = 25) and CTSC-*LIN* (n = 25) at the time of myocardial infarction surgery together with EdU mini-pump implantation that was removed at D7. Hearts were harvested at D2 and D7 for histology and RNA analysis. Animals were analyzed for echos/hemodynamic measurements, histology and RNA analysis at terminal time point i.e., 8 weeks after MI. B) Increased ejection fraction and fractional shortening (C) in CTSC-*LIN* (n = 10) administered hearts compared to CTSC-*GFP* (n = 10) and PBS (n = 10) animals at 8 weeks after MI. D) Speckle-tracking based strain imaging; Three-dimensional regional wall velocity diagrams show contraction (orange/positive values) or relaxation (blue/negative values) of consecutive cardiac cycles 8 weeks after MI. Vector diagrams show the direction and magnitude of endocardial contraction at mid-systole 8 weeks after MI. E-F) Apical and global longitudinal strain, G-H) Apical and global longitudinal strain rate. (n = 10/group) I-J) Hemodynamic measurements show increased dp/dtmax and reduced dp/dtmin and K-L) LVEDP and heart rate 8 weeks after MI (n = 3/group). CTSC-*LIN* vs. PBS $^{*}p<0.05$, $^{**}p<0.01$, $^{***}p<0.001$, CTSC-*LIN* vs CTSC-*GFP* $^{\#}p<0.05$, $^{\#\#}p<0.01$, $^{\#\#\#}p<0.001$. (For interpretation of the references to color in this figure legend, the reader is referred to the Web version of this article.)

and compared it to metabolic genes altered in CTSC-*LIN* to identify common genes. This analysis demonstrated pyruvate dehydrogenase kinase 1 (PDK1) as one of the top let-7 target genes altered in CTSC-*LIN*. Further validation confirmed increased levels of PDK1 and other family members such as PDK4 in CTSC-*LIN* (Fig. 4C and D). Additionally, treatment of CTSC-*LIN* with let-7 mimic reduced mRNA expression of PDK1, PDK4 and HK2 while let-7 antimiR showed marked increase (Fig. 4E). Next, CTSC-*LIN* were infected with sh-PDK1 to block PDK1 expression (Fig. 4F and G) followed by analysis of proliferation. Results showed complete blockade of cell proliferation in CTSC-*LIN* after sh-PDK1 compared to control cells as measured by CyQuant assay (Fig. 4H). Similarly, pharmacological blockade of PDK1 by dichloroacetate and 3-bromopyruvate in CTSC-*LIN* reduced PDK1decreasing phosphorylation of PDHE1α^{S293} subunit that was highly phosphorylated in CTSC-*LIN* and regulates pyruvate entry into mitochondria (Fig. 4I) together with complete abrogation of cell proliferation (Fig. 4J). Taken together, results show LIN28a effects on proliferation are in part dependent on the let-7/PDK1 signaling pathway.

LIN28a CTSCs augment cardiac structure and function after myocardial ischemic injury. To assess whether LIN28a modified adult CTSCs are a viable therapeutic option for cardiac repair after myocardial injury, both CTSC-*LIN* *and* CTSC-*GFP* were transplanted in the heart after myocardial infarction (MI) injury followed by functional and histological assessments at day 2, day7 and 8 weeks after MI (Fig. 5A). Left ventricular function showed increased ejection fraction (Fig. 5B) and fractional shortening (Fig. 5C and Online Fig. 5A and B) was observed in CTSC-*LIN* animals compared to CTSC-*LIN* and PBS control hearts 8 weeks after MI together with increase left ventricular anterior wall thickness (LVAW) (Online Fig. 5C) and reduced left ventricular internal diameter (LVID) (Online Fig. 5D). Additionally, speckle-tracking based strain analysis on echocardiography B-mode loops was performed and Fig. 5D shows three-dimensional regional wall velocity diagrams and vector diagrams for all 3 groups, respectively, 8 weeks after myocardial infarction and cell transplantation. Analysis of apical and longitudinal strain and rates showed significant improvement in animals transplanted with CTSC-*LIN* compared to CTSC-*GFP* and PBS animals 8 weeks after MI (Fig. 5E–H). Hemodynamic measurements showed increased cardiac contractility in CTSC-*LIN* heart compared to controls animals 8 weeks after MI and no change in heart rate during measurements for mice in all groups (Fig. 5I–L). In parallel, CTSC-*LIN* administered hearts showed decrease infarct size at 8 weeks (Online Fig. 6A) and apoptosis at day 2 (Online Fig. 6B) after injury compared to both CTSC-*GFP* and PBS control animals. Analysis of myocyte size (Online Fig. 6C) and HW/BW ratio (Online Fig. 6D) showed significant reduction in CTSC-*LIN* transplanted hearts and increased number of small myocytes in border zone (Online Fig. 6E) compared to control animals together reduction in markers of hypertrophy (Online Fig. 6F) 8 weeks after MI.

Enhanced survival and proliferation of LIN28a modified CTSCs in the ischemic heart. Cell-based therapies have typically underperformed due inability of the cells to survive in the ischemic heart with less than 1% cells post 24 h after adoptive transfer [7]. To test whether LIN28a modification increases CTSC persistence in the heart, cells were

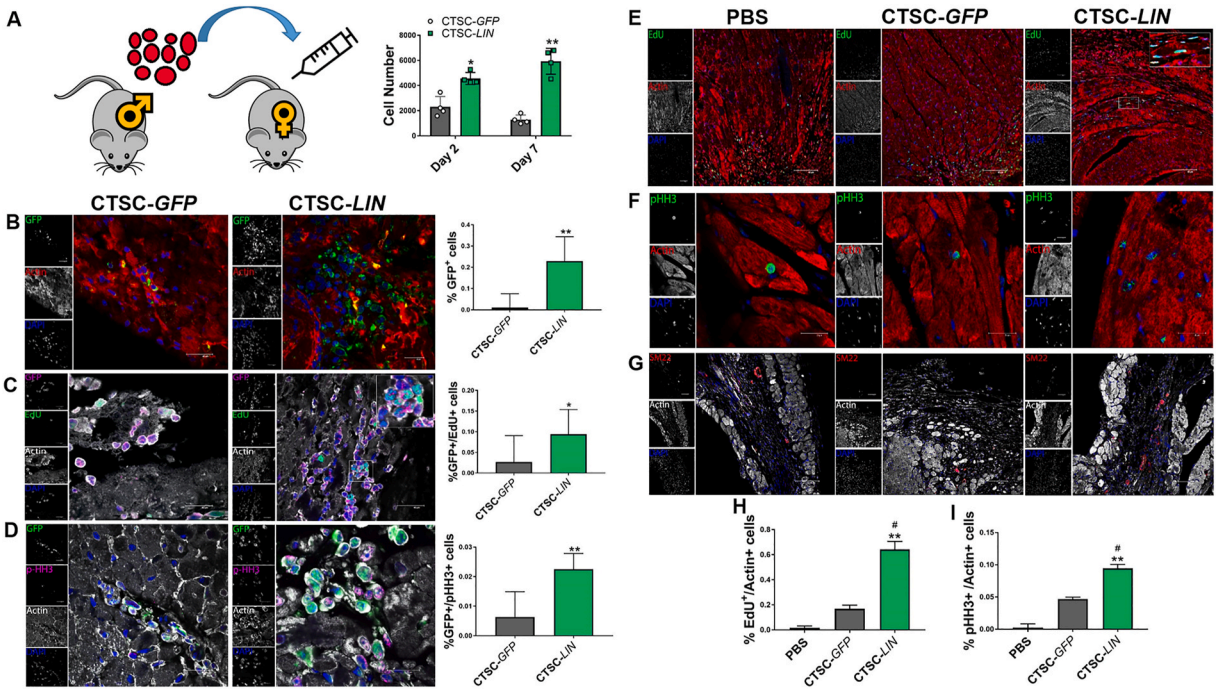

Fig. 6. Increase survival, proliferation and pro-reparative effects of CTSC-*LIN* in the heart post ischemic injury. A) Female mice with acute MI received male 1×10^5 CTSC-*LIN* or CTSC-*GFP*. Hearts were extracted at day 2 and 7 and hPBMCs internal standard was added before isolation of genomic DNA followed by Rbmy quantification by PCR and cell number calculations. (n = 3 animals/day 2 and day7/cell line). B) Histological analysis of heart sections reveals increased GFP + cells 2 days in the border zone area after MI in CTSC-*LIN* group compared to controls along with quantification. GFP (green), Actin (red) and nuclei (blue), scale bar = 40 μm. (n = 6). C) Increased GFP+/EdU + cells in CTSC-*LIN* hearts compared to controls 2 days after MI along with quantification. GFP (pink), EdU (green), actin (white) nuclei (blue). Scale bar = 40 μm. (n = 6). D) Increased GFP+/pHH3+ cells in CTSC-*LIN* hearts compared to controls 2 days after MI along with quantification. GFP (green), p-HH3 (pink), actin (white) nuclei (blue). Scale bar = 20 μm. (n = 6). E) EdU detection of the hearts at 8 weeks showed high number of EdU+/Actin + cells in CTSC-*LIN* group compared to control along with quantification (H) (n = 8). EdU (green), actin (red), nuclei (blue), scale bar = 40 μm. F) Increased number of p-histone 3+/Actin + myocytes in the CTSC- *LIN* hearts compared to CTSC-*GFP* and PBS administered control 8 weeks after MI along with quantification (I). p-HH3 (green), Actin (red), nuclei (blue). Scale bar = 20 μm (n = 8/group). G) Increased SM22+ cells in CTSC- *LIN* in the heart 8 weeks after MI compared to controls. SM22 (red), Actin (white), nuclei (blue). Scale bar = 40 μm (n = 8/group). CTSC-*LIN* vs. PBS $^{*}p<0.05$, $^{**}p<0.01$, $^{***}p<0.001$, CTSC-*LIN* vs CTSC-*GFP* $^{\#}p<0.05$, $^{\#\#}p<0.01$, $^{\#\#\#}p<0.001$. (For interpretation of the references to color in this figure legend, the reader is referred to the Web version of this article.)

isolated from male hearts, infected with LIN28a or GFP only lentivirus and transplanted in a female heart followed by PCR based quantification of cell numbers at day 2 and day 7 post transplantation as described previously [7]. Analysis of 1×10^5 cell transplanted for presence of male *Rbmy* gene (Online Fig. 7A and B), showed about 4% CTSC-*LIN* cells surviving at day 2 which increased to 6% at day 7 post transplantation while CTSC-*GFP* only showed 2% and 1% survival rates respectively (Fig. 6A). Immunohistochemical analysis of the hearts showed increased GFP + cells in CTSC-*LIN* transplanted animals compared to CTSC-*GFP* control animals 2 days post transplantation (Fig. 6B). Similarly, CTSC-LIN cells showed significant proliferation as evidenced by increased GFP+/EdU+ (Fig. 6C) and GFP+/pHH3+ (Fig. 6D) 2 days after transplantation compared to CTSC-*GFP*. Additionally, LIN28a mRNA (Online Fig. 7C) expression was elevated while let-7 decreased (Online Fig. 7D) in the CTSC-LIN hearts 2 days after injury together with increased expression of cell cycle markers (Online Fig. 7E) and glycolytic genes (Online Fig. 7F) 7 days after MI compared to CTSC-*GFP* and PBS administered animals. Finally, glycolytic induction in CMs after CTSC-LIN transplantation was assessed by seahorse assay. Increased ECAR in isolated adult cardiomyocytes 7 days after injury and cell transplantation in animals administered CTSC-*LIN* as compared to CTSC-*GFP* (Online Fig. 7G).

To determine the functional consequence of increased CTSC-*LIN* cells in the heart, it was hypothesized that CTSC-*LIN* potentially promote cardiomyocyte (CM) cell cycle activity and survival in the heart 8 weeks post injury. To test this hypothesis, heart sections from CTSC-*LIN* transplanted animals were stained for EdU and showed increased EdU+/Actin + cells 8 weeks after MI compared to CTSC-*GFP* and PBS animals (Fig. 6E,H). Similarly, increased pHH3+/Actin+ in the CTSC-*LIN* hearts compared to control animals after 8 weeks of injury (Fig. 6F,I). Finally, CTSC-LIN transplantation led to significantly increased SM22+ new blood vessel formation in the heart 8 weeks after MI compared to control hearts (Fig. 6G).

Metabolic reprogramming alters CTSC secretory properties and cardiomyocyte proliferation. Recent studies indicate that stem cells salutary effects are tied to ability to release pro-reparative paracrine factors at the site of injury [22,28]. Therefore, whether LIN28a mediated metabolic reprogramming alters ability of adult CTSCs to secrete various growth factors was tested. Results show that CTSC-*LIN* possess increased ability to secrete pro-reparative growth factors such as *IGF-1, SDF-1, VEGF* and *HGF* in comparison to control cells under 5% hypoxia growth conditions as confirmed by immunocytochemistry (Fig. 7A) and mRNA expression in part due to increase in cell number (Fig. 7B). Additionally, treatment of CTSC-LIN 2-deoxyglucose (2-DG), inhibitor for glycolysis (Fig. 7C) or let-7 mimic (Fig. 7D) under hypoxia conditions significantly reduced the ability of CTSC-LIN to produce various growth factors while antimycin A, inhibitor for oxidative phosphorylation treatment reversed the results. Next, whether increased ability to secrete growth factors by CTSC-*LIN* alters CM survival or proliferation was assessed. For this purpose, media from CTSC-*LIN* and CTSC-*GFP* cultured under normoxia and hypoxia condition was harvested and plated on top of neonatal rat ventricular myocytes (NRVMs). Media from CTSC-*LIN* under hypoxia significantly increased cell cycle marker Ki67+ in NRVMs compared to normoxia or CTSC-*GFP* media (Fig. 7E). Additionally, NRVMs were subjected to H2O2 stress followed by treatment with CTSC-*LIN* and CTSC-*LIN* media under hypoxia. CTSC-*LIN* media

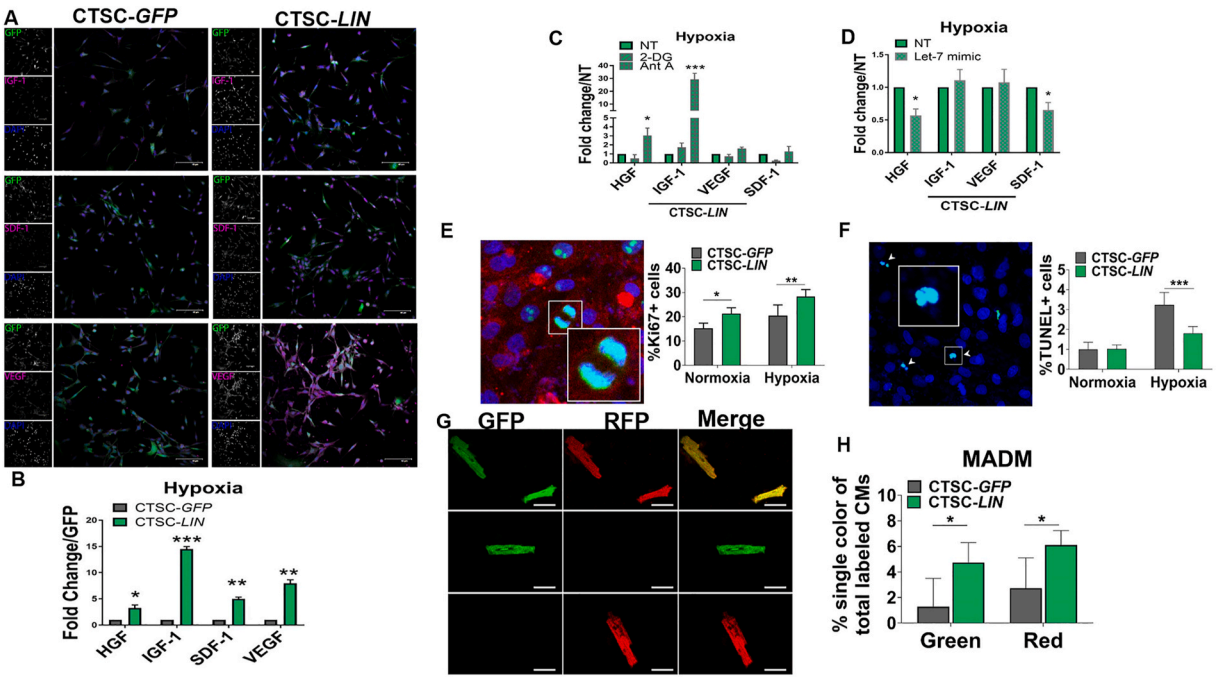

Fig. 7. LIN28a promotes paracrine activity in CTSCs that drives cardiomyocyte cell cycle and survival. A) Increased expression of IGF-1, SDF-1 and VEGF in CTSC-*LIN* compared to CTSC-*GFP* after 48hrs of 5%hypoxia treatment. (n = 3) GFP (green), IGF1/SDF-1/VEGF (pink), nuclei (blue). Scale bar = 40 μm. B) mRNA expression analysis for growth factors in CTSC-*LIN* and CTSC-*GFP* after 48hrs of 5%hypoxia treatment. (n = 4). C) mRNA analysis for growth factors in CTSC-*LIN* and CTSC-*GFP* after 48hrs treatment with antimycin-A (Act-A) and 2-deoxyglucose (2-DG). (n = 3). D) Treatment with Let-7 mimic for 48hrs reduces growth factor mRNA expression in CTSC-*LIN*. (n = 3). Increased Ki67+ actinin + cells (E) and decreased TUNEL + cells (F) after 24hrs treatment with media harvested from normoxic and hypoxic CTSC-*LIN* cells compared to controls. (n = 4). G) Representative immunofluorescence images of single colored (red or green) cells, indicating cells that underwent cytokinesis in isolated cardiomyocytes from cre-inducted MADM mice (4-month-old) 4 weeks after CTSC-*LIN*/CTSC-*GFP* transplantation. (n = 3–4 animals in each group, (400K cells analyzed/group) along with quantification (H). CTSC-*LIN* vs CTSC-*GFP* $*p<0.05$, $**p<0.01$, $***p<0.001$. (For interpretation of the references to color in this figure legend, the reader is referred to the Web version of this article.)

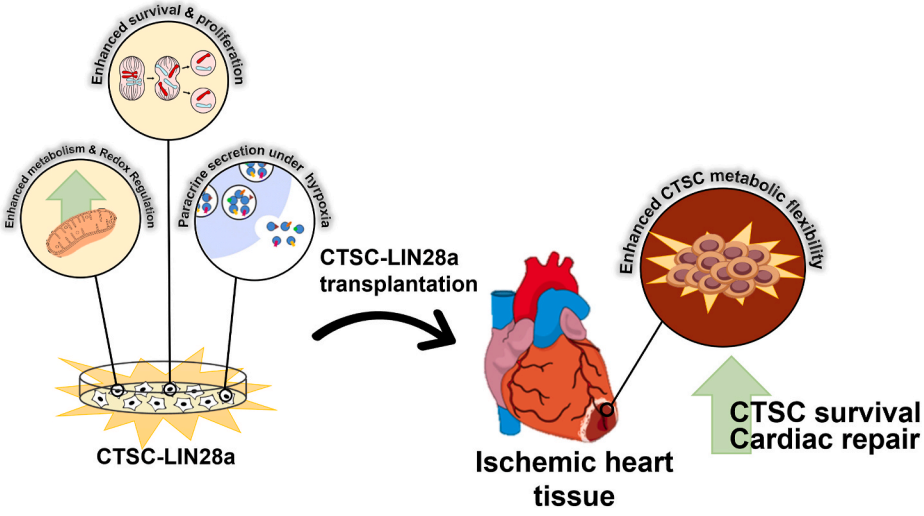

Fig. 8. Schematic representation of the working hypothesis. Adult CTSCs engineered with LIN28a exhibit reprogrammed metabolism, redox regulation and enhanced survival/proliferation and paracrine secretion. Following transplantation, CTSC-*LIN* show increased survival and ability to the repair the heart after myocardial ischemic injury due to LIN28a induced metabolic flexibility in response to near anoxia in the heart.

under hypoxia significantly reduced TUNEL + cells in NRVMs compared to CTSC-*LIN* media treated cells (Fig. 7F). Finally, we utilized double mosaic lineage tracing (MADM) mouse model system to validate ability of CTSC-*LIN* to drive new CM formation in the heart. For this purpose, CTSC-*LIN and* CTSC-*GFP* were transplanted in the hearts of MADM mice at the time of myocardial infarction injury. Animals were followed for 4 weeks after which hearts were digested to isolated single CMs while GFP + CTSC were not collected since the MADM system does not label CTSCs. CTSC-*LIN* transplanted hearts showed significant increase in green and red colored CMs compared to CTSC-*GFP* administered hearts 4 weeks after MI indicating new myocyte formation (Fig. 7G and H). These results show that LIN28a modification of adult CTSCs changes ability to secrete pro-reparative growth factors that promote new cardiomyocyte formation in the heart after injury (see Fig. 8).

4. Discussion

Our findings here link modulation of cellular metabolism as a strategy to increase survival and proliferation of cardiac tissue derived stem like cells (CTSCs) in heart after ischemic injury. Additionally, our data identifies therapeutic value of developmental metabolic regulator LIN28a in CTSCs for cardiac repair by promoting 'metabolic flexibility', defined as the ability to switch to glycolysis for energy generation in response to decreased oxygen levels in the heart post ischemic injury and under ambient oxygen and growth conditions, increasing both ECAR and oxidative phosphorylation for rapid proliferation.

Developmental mammalian heart is a proliferative organ capable of regenerating itself after injury [29]. Studies have shown existence of cardiac progenitors in the developmental heart that give rise to multiple cardiac lineages [30] and isolation of cardiac stem/progenitors from the developmental cardiac tissue reveals strong regenerative properties [31]. In the adult heart however, existence of stem/progenitor cells population and their ability to form cardiomyocytes has become controversial lately [32]. Yet, these studies confirm a cell population exhibiting stem cell markers while its precise role in the heart remains to be elucidated. Interestingly, regenerative potential of the developmental heart is linked to the presence of a unique metabolic phenotype that is altered as the heart loses ability to regenerate [33]. Reintroduction of developmental factors in the adult heart has been an attractive choice lately enhancing cardiac structure and function [34]. Nevertheless, whether there are developmental metabolic regulators with ability to promote cardiac cell potential to repair the heart remains untested.

We have recently identified a novel developmental miR-294 based signaling complex in the heart that drives cardiac repair after injury [19]. Our results show that miR-294 expression is synonymous with RNA binding protein LIN28a in the heart in concordance with previous studies identifying LIN28a as a downstream target of miR-294 [35]. Our prior work shows enhanced LIN28a expression in newly identified cardiac tissue derived stem like cells (CTSCs) in the heart of neonatal mice while aged CTSCs lose LIN28a expression [2]. The precise role of LIN28a in CTSCs remains unknown and whether adult CTSC modified with LIN28a demonstrate increased functional properties has never been tested. Therefore, we provide here a novel role for developmental factor LIN28a in enhancing cardiac cell function for repair of ischemic heart. LIN28a has been identified as master regulator of growth and metabolism [24] and is highly expressed during development and in pluripotent stem cells regulating core function such as pluripotency, self-renewal and proliferation [24]. Reintroduction of LIN28a in adult tissues is associated with increased tissue regeneration after injury [25]. Mechanistically, LIN28a represses Let-7 expression thereby regulating let-7 target genes [27] but also directly binds to other mRNAs modulating gene expression in let-7 independent manner [25]. LIN28a expression is associated with increased glycolytic flux and pentose phosphate pathway that together enhances cellular proliferation. Concurrently, our results show that modification of adult CTSCs with LIN28a increases glycolytic metabolites and intermediates, enzymes and cellular proliferation. This LIN28a mediated enhancement of cellular function was linked to let-7 dependent targeting of pyruvate dehydrogenase kinase (PDK1) in concurrence with Ma and colleagues who found cancer cell proliferation is dependent on LIN28a targeting of let-7 target gene PDK-1 and thereby promoting aerobic glycolysis [36]. Additionally, metabolome profiling identified glycolytic intermediates that fuel the pentose phosphate pathway (PPP). Prior studies have identified a beneficial role for increased PPP for enhancement of cardiac progenitor cell function thereby supporting our findings and highlighting the importance of glycolytic signaling, PPP and increased proliferation rates [37]. Taken together, our findings here suggest that introduction of LIN28a in adult CTSCs via modulation of various let-7 metabolic target genes promotes glycolysis supporting increased proliferation and functional CTSC properties.

Reduced oxygen levels or 'near anoxia' are the primary cause of injury in the heart that leads to cardiomyocyte loss and scar formation. Cell-based therapeutics have been widely applied for resolution of cardiac injury yet have underperformed due massive cell lose following adoptive transfer [9]. Ex vivo expansion under ambient oxygen is necessary for cell-based therapies to obtain required cell numbers for adoptive transfer but drives metabolism towards oxidative phosphorylation, increased ROS levels and reduced stem cell like properties [11]. Consequently, adoptive transfer strategies encounter massive cell loss following transplantation due inability of the donated cells to metabolically adapt to ischemic or near anoxia conditions in the heart [11]. Various strategies have been employed to enhance cell survival post transplantation such as genetic modification [38,39], growth factor pretreatment [40] and pharmacological treatments [41,42], hypoxia [43], etc. Nevertheless, promoting metabolic flexibility in ex vivo expanded cardiac cells to enhance ability to survive and repair the heart after injury has never been tested. Our findings show that LIN28a modification of adult CTSCs increases survival rate to 6% 7 days post transplantation in the heart after myocardial infarction. We believe that this increase in survival is the direct consequence of LIN28a mediated switching of metabolism to glycolysis, reducing ROS generation in low-oxygen environment typical of cardiac injury. Concurrently, Derlet et al., identified cellular metabolism as a determinant of cell therapy efficacy [44]. Authors showed increasing glycolysis and reducing respiration without affecting total ATP-generation increased functional properties of hematopoietic stem progenitor cells and bone marrow cells. Similarly, hypoxic preconditioning of mesenchymal stromal cells led to metabolic changes together with increased survival and retention following in vivo transplantation [43], thereby suggesting metabolism as a determinant of cell therapy effectiveness. Another unique feature of the study is the finding that LIN28a adult CTSCs demonstrate increased cardiomyocyte cell proliferation in the heart after injury providing a novel link between metabolism and paracrine secretion by adoptively transferred stem cells. Therefore, salutary effects of CTSC-*LIN* on cardiac function are tied to the enhanced ability of cells to survive and proliferate immediately after transplantation that leads to greater accumulation of pro-regenerative factors in the heart activating cardiomyocyte proliferation following injury.

In conclusion, our findings here identify a novel role for RNA-binding protein LIN28a in cardiac repair after ischemic injury. Modification of CTSCs with LIN28a promotes metabolic flexibility increasing ability to survive and proliferate in the heart under near anoxia together with enhancement of cardiac structure and function following myocardial infarction.

Declaration of competing interest

I declare that there are no conflicts of interest.

Acknowledgements

We thank all members of the Khan laboratory for their valuable discussions as well Temple Flow Cytometry core. This work was supported by National Institute of Health grant HL135177 and H1801 WW Smith Charitable Trust to M. Khan and HL137850 and 15SDG25550038 to S. Mohsin.

Appendix A. Supplementary data

Supplementary data to this article can be found online at https://doi.org/10.1016/j.redox.2021.102162.

References

[1] O. Bergmann, S. Zdunek, A. Felker, M. Salehpour, K. Alkass, S. Bernard, S. L. Sjostrom, M. Szewczykowska, T. Jackowska, C. Dos Remedios, T. Malm, M. Andra, R. Jashari, J.R. Nyengaard, G. Possnert, S. Jovinge, H. Druid, J. Frisen,

Dynamics of cell generation and turnover in the human heart, Cell 161 (7) (2015) 1566–1575.
[2] J. Kurian, A.E. Yuko, N. Kasatkin, V.O.C. Rigaud, K. Busch, D. Harlamova, M. Wagner, F.A. Recchia, H. Wang, S. Mohsin, S.R. Houser, M. Khan, Uncoupling protein 2-mediated metabolic adaptations define cardiac cell function in the heart during transition from young to old age, Stem Cells Transl Med 10 (1) (2020) 144–156.
[3] R.R. Smith, L. Barile, H.C. Cho, M.K. Leppo, J.M. Hare, E. Messina, A. Giacomello, M.R. Abraham, E. Marban, Regenerative potential of cardiosphere-derived cells expanded from percutaneous endomyocardial biopsy specimens, Circulation 115 (7) (2007) 896–908.
[4] K.L. Laugwitz, A. Moretti, J. Lam, P. Gruber, Y. Chen, S. Woodard, L.Z. Lin, C. L. Cai, M.M. Lu, M. Reth, O. Platoshyn, J.X. Yuan, S. Evans, K.R. Chien, Postnatal isl 1+ cardioblasts enter fully differentiated cardiomyocyte lineages, Nature 433 (7026) (2005) 647–653.
[5] C.M. Martin, A.P. Meeson, S.M. Robertson, T.J. Hawke, J.A. Richardson, S. Bates, S. C. Goetsch, T.D. Gallardo, D.J. Garry, Persistent expression of the ATP-binding cassette transporter, Abcg2, identifies cardiac SP cells in the developing and adult heart, Dev. Biol. 265 (1) (2004) 262–275.
[6] P.P. Zwetsloot, A.M. Vegh, S.J. Jansen of Lorkeers, G.P. van Hout, G.L. Currie, E. S. Sena, H. Gremmels, J.W. Buikema, M.J. Goumans, M.R. Macleod, P. A. Doevendans, S.A. Chamuleau, J.P. Sluijter, Cardiac stem cell treatment in myocardial infarction: a systematic review and meta-analysis of preclinical studies, Circ. Res. 118 (8) (2016) 1223–1232.
[7] K.U. Hong, Q.H. Li, Y. Guo, N.S. Patton, A. Moktar, A. Bhatnagar, R. Bolli, A highly sensitive and accurate method to quantify absolute numbers of c-kit+ cardiac stem cells following transplantation in mice, Basic Res. Cardiol. 108 (3) (2013) 346.
[8] J.S. Forrester, P. Libby, The inflammation hypothesis and its potential relevance to statin therapy, Am. J. Cardiol. 99 (5) (2007) 732–738.
[9] J. Dow, B.Z. Simkhovich, L. Kedes, R.A. Kloner, Washout of transplanted cells from the heart: a potential new hurdle for cell transplantation therapy, Cardiovasc. Res. 67 (2) (2005) 301–307.
[10] K. Ito, T. Suda, Metabolic requirements for the maintenance of self-renewing stem cells, Nat. Rev. Mol. Cell Biol. 15 (4) (2014) 243–256.
[11] G.E. Salazar-Noratto, G. Luo, C. Denoeud, M. Padrona, A. Moya, M. Bensidhoum, R. Bizios, E. Potier, D. Logeart-Avramoglou, H. Petite, Understanding and leveraging cell metabolism to enhance mesenchymal stem cell transplantation survival in tissue engineering and regenerative medicine applications, Stem Cell. 38 (1) (2020) 22–33.
[12] Q. Wu, Q. Liu, J. Zhan, Q. Wang, D. Zhang, S. He, S. Pu, Z. Zhou, Cited 2 regulates proliferation and survival in young and old mouse cardiac stem cells, BMC Mol Cell Biol 20 (1) (2019) 25.
[13] W.E. Wang, D. Yang, L. Li, W. Wang, Y. Peng, C. Chen, P. Chen, X. Xia, H. Wang, J. Jiang, Q. Liao, Y. Li, G. Xie, H. Huang, Y. Guo, L. Ye, D.D. Duan, X. Chen, S. R. Houser, C. Zeng, Prolyl hydroxylase domain protein 2 silencing enhances the survival and paracrine function of transplanted adipose-derived stem cells in infarcted myocardium, Circ. Res. 113 (3) (2013) 288–300.
[14] A. Moussaieff, M. Rouleau, D. Kitsberg, M. Cohen, G. Levy, D. Barasch, A. Nemirovski, S. Shen-Orr, I. Laevsky, M. Amit, D. Bomze, B. Elena-Herrmann, T. Scherf, M. Nissim-Rafinia, S. Kempa, J. Itskovitz-Eldor, E. Meshorer, D. Aberdam, Y. Nahmias, Glycolysis-mediated changes in acetyl-CoA and histone acetylation control the early differentiation of embryonic stem cells, Cell Metabol. 21 (3) (2015) 392–402.
[15] N. Shyh-Chang, H.H. Ng, The metabolic programming of stem cells, Genes Dev. 31 (4) (2017) 336–346.
[16] J. Zhang, E. Nuebel, G.Q. Daley, C.M. Koehler, M.A. Teitell, Metabolic regulation in pluripotent stem cells during reprogramming and self-renewal, Cell Stem Cell 11 (5) (2012) 589–595.
[17] F. Sanada, J. Kim, A. Czarna, N.Y. Chan, S. Signore, B. Ogorek, K. Isobe, E. Wybieralska, G. Borghetti, A. Pesapane, A. Sorrentino, E. Mangano, D. Cappetta, C. Mangiaracina, M. Ricciardi, M. Cimini, E. Ifedigbo, M.A. Perrella, P. Goichberg, A.M. Choi, J. Kajstura, T. Hosoda, M. Rota, P. Anversa, A. Leri, c-Kit-positive cardiac stem cells nested in hypoxic niches are activated by stem cell factor reversing the aging myopathy, Circ. Res. 114 (1) (2014) 41–55.
[18] W. Kimura, H.A. Sadek, The cardiac hypoxic niche: emerging role of hypoxic microenvironment in cardiac progenitors, Cardiovasc. Diagn. Ther. 2 (4) (2012) 278–289.
[19] A. Borden, J. Kurian, E. Nickoloff, Y. Yang, C.D. Troupes, J. Ibetti, A.M. Lucchese, E. Gao, S. Mohsin, W.J. Koch, S.R. Houser, R. Kishore, M. Khan, Transient introduction of miR-294 in the heart promotes cardiomyocyte cell cycle reentry after injury, Circ. Res. 125 (1) (2019) 14–25.
[20] M.S. Choudhery, M. Khan, R. Mahmood, S. Mohsin, S. Akhtar, F. Ali, S.N. Khan, S. Riazuddin, Mesenchymal stem cells conditioned with glucose depletion augments their ability to repair-infarcted myocardium, J. Cell Mol. Med. 16 (10) (2012) 2518–2529.
[21] M. Khan, S. Mohsin, D. Avitabile, S. Siddiqi, J. Nguyen, K. Wallach, P. Quijada, M. McGregor, N. Gude, R. Alvarez, D.G. Tilley, W.J. Koch, M.A. Sussman, beta-Adrenergic regulation of cardiac progenitor cell death versus survival and proliferation, Circ. Res. 112 (3) (2013) 476–486.
[22] M. Khan, E. Nickoloff, T. Abramova, J. Johnson, S.K. Verma, P. Krishnamurthy, A. R. Mackie, E. Vaughan, V.N. Garikipati, C. Benedict, V. Ramirez, E. Lambers, A. Ito, E. Gao, S. Misener, T. Luongo, J. Elrod, G. Qin, S.R. Houser, W.J. Koch, R. Kishore, Embryonic stem cell-derived exosomes promote endogenous repair mechanisms and enhance cardiac function following myocardial infarction, Circ. Res. 117 (1) (2015) 52–64.
[23] J.M. Duran, C.A. Makarewich, T.E. Sharp, T. Starosta, F. Zhu, N.E. Hoffman, Y. Chiba, M. Madesh, R.M. Berretta, H. Kubo, S.R. Houser, Bone-derived stem cells repair the heart after myocardial infarction through transdifferentiation and paracrine signaling mechanisms, Circ. Res. 113 (5) (2013) 539–552.
[24] N. Shyh-Chang, G.Q. Daley, Lin28: primal regulator of growth and metabolism in stem cells, Cell Stem Cell 12 (4) (2013) 395–406.
[25] N. Shyh-Chang, H. Zhu, T. Yvanka de Soysa, G. Shinoda, M.T. Seligson, K. M. Tsanov, L. Nguyen, J.M. Asara, L.C. Cantley, G.Q. Daley, Lin28 enhances tissue repair by reprogramming cellular metabolism, Cell 155 (4) (2013) 778–792.
[26] V.O.C. Rigaud, R. Hoy, S. Mohsin, M. Khan, Stem cell metabolism: powering cell-based therapeutics, Cells 9 (11) (2020).
[27] D. Ustianenko, H.S. Chiu, T. Treiber, S.M. Weyn-Vanhentenryck, N. Treiber, G. Meister, P. Sumazin, C. Zhang, LIN28 selectively modulates a subclass of let-7 MicroRNAs, Mol. Cell 71 (2) (2018) 271–283 e5.
[28] R. Kishore, M. Khan, More than tiny sacks: stem cell exosomes as cell-free modality for cardiac repair, Circ. Res. 118 (2) (2016) 330–343.
[29] E.R. Porrello, A.I. Mahmoud, E. Simpson, J.A. Hill, J.A. Richardson, E.N. Olson, H. A. Sadek, Transient regenerative potential of the neonatal mouse heart, Science 331 (6020) (2011) 1078–1080.
[30] T.Y. de Soysa, S.S. Ranade, S. Okawa, S. Ravichandran, Y. Huang, H.T. Salunga, A. Schricker, A. Del Sol, C.A. Gifford, D. Srivastava, Single-cell analysis of cardiogenesis reveals basis for organ-level developmental defects, Nature 572 (7767) (2019) 120–124.
[31] D.L. Simpson, R. Mishra, S. Sharma, S.K. Goh, S. Deshmukh, S. Kaushal, A strong regenerative ability of cardiac stem cells derived from neonatal hearts, Circulation 126 (11 Suppl 1) (2012) S46–S53.
[32] J.H. van Berlo, O. Kanisicak, M. Maillet, R.J. Vagnozzi, J. Karch, S.C. Lin, R. C. Middleton, E. Marban, J.D. Molkentin, c-kit+ cells minimally contribute cardiomyocytes to the heart, Nature 509 (7500) (2014) 337–341.
[33] A. de Carvalho, V. Bassaneze, M.F. Forni, A.A. Keusseyan, A.J. Kowaltowski, J. E. Krieger, Early postnatal cardiomyocyte proliferation requires high oxidative energy metabolism, Sci. Rep. 7 (1) (2017) 15434.
[34] V.O.C. Rigaud, M. Khan, Aging in reverse: reactivating developmental signaling for cardiomyocyte proliferation, J. Mol. Cell. Cardiol. 154 (2021) 1–5.
[35] K. Yuan, W.B. Ai, L.Y. Wan, X. Tan, J.F. Wu, The miR-290-295 cluster as multi-faceted players in mouse embryonic stem cells, Cell Biosci. 7 (2017) 38.
[36] X. Ma, C. Li, L. Sun, D. Huang, T. Li, X. He, G. Wu, Z. Yang, X. Zhong, L. Song, P. Gao, H. Zhang, Lin28/let-7 axis regulates aerobic glycolysis and cancer progression via PDK1, Nat. Commun. 5 (2014) 5212.
[37] R. Katare, A. Caporali, C. Emanueli, P. Madeddu, Benfotiamine improves functional recovery of the infarcted heart via activation of pro-survival G6PD/Akt signaling pathway and modulation of neurohormonal response, J. Mol. Cell. Cardiol. 49 (4) (2010) 625–638.
[38] S. Mohsin, M. Khan, H. Toko, B. Bailey, C.T. Cottage, K. Wallach, D. Nag, A. Lee, S. Siddiqi, F. Lan, K.M. Fischer, N. Gude, P. Quijada, D. Avitabile, S. Truffa, B. Collins, W. Dembitsky, J.C. Wu, M.A. Sussman, Human cardiac progenitor cells engineered with Pim-I kinase enhance myocardial repair, J. Am. Coll. Cardiol. 60 (14) (2012) 1278–1287.
[39] M. Khan, S. Mohsin, H. Toko, M. Alkatib, J. Nguyen, S. Truffa, N. Gude, K. Chuprun, D.G. Tilley, W.J. Koch, M.A. Sussman, Cardiac progenitor cells engineered with betaARKct have enhanced beta-adrenergic tolerance, Mol. Ther. 22 (1) (2014) 178–185.
[40] H. Haider, S. Jiang, N.M. Idris, M. Ashraf, IGF-1-overexpressing mesenchymal stem cells accelerate bone marrow stem cell mobilization via paracrine activation of SDF-1 alpha/CXCR4 signaling to promote myocardial repair, Circ. Res. 103 (11) (2008) 1300–1308.
[41] M. Ali, A. Mehmood, M.S. Anjum, M.N. Tarrar, S.N. Khan, S. Riazuddin, Diazoxide preconditioning of endothelial progenitor cells from streptozotocin-induced type 1 diabetic rats improves their ability to repair diabetic cardiomyopathy, Mol. Cell. Biochem. 410 (1–2) (2015) 267–279.
[42] D. Han, X. Li, W.S. Fan, J.W. Chen, T.T. Gou, T. Su, M.M. Fan, M.Q. Xu, Y.B. Wang, S. Ma, Y. Qiu, F. Cao, Activation of cannabinoid receptor type II by AM1241 protects adipose-derived mesenchymal stem cells from oxidative damage and enhances their therapeutic efficacy in myocardial infarction mice via Stat 3 activation, Oncotarget 8 (39) (2017) 64853–64866.
[43] J. Beegle, K. Lakatos, S. Kalomoiris, H. Stewart, R.R. Isseroff, J.A. Nolta, F. A. Fierro, Hypoxic preconditioning of mesenchymal stromal cells induces metabolic changes, enhances survival, and promotes cell retention in vivo, Stem Cell. 33 (6) (2015) 1818–1828.
[44] A. Derlet, T. Rasper, A. Roy Choudhury, S. Bothur, M.A. Rieger, D. Namgaladze, A. Fischer, C. Schurmann, R.P. Brandes, U. Tschulena, S. Steppan, B. Assmus, S. Dimmeler, A.M. Zeiher, F.H. Seeger, Metabolism regulates cellular functions of bone marrow-derived cells used for cardiac therapy, Stem Cell. 34 (8) (2016) 2236–2248.